Modal-Space Active Damping of a Plane Grid: Experiment and Theory

Wm. L. Hallauer Jr.,* Gary R. Skidmore,† and Russell N. Gehling†
Virginia Polytechnic Institute and State University, Blacksburg, Virginia

This paper first reviews a theory of multiple-actuator modal-space active damping (control) which uses spectral filtering for modal estimation; then it describes an experiment in which the control technique was applied in analog form to a laboratory plane grid structure having a dozen modes under 10 Hz. Experimental observations and corresponding theoretical calculations are presented. Active damping of five modes, including a closely spaced pair, was attempted with the use of five control actuators. However, coupling between the two close modes and their filters produced a mild system instability. Subsequently, a stable four-mode controller was produced by disabling the control of the mode that had driven the instability. The spectral filtering played an unexpectedly dominant and counterproductive role in the active damping process.

I. Introduction

THIS paper pertains to the active damping (control) of structural vibration, excluding self-excited vibration such as aeroelastic flutter. As preparations are made for greatly expanded operations in Earth orbit, the dynamics and control of highly flexible satellites become increasingly important. The anticipated application of the type of active damping considered in this paper is vibration control of large space structures.

In the past several years, there have been many studies of active vibration damping. Most have been purely theoretical, but recently an increasing number of experimental studies have been reported (see, for example, Refs. 1-7). Most previous reports of experimental studies either have not presented comparisons of experimental data with corresponding theoretical calculations or have presented only very limited comparisons. But experimental-theoretical comparisons are required in order to either validate theoretical concepts for practical application or reveal the factors that prevent evidently promising theoretical concepts from being successful in practice. Therefore, the present authors' general objectives are to design and execute experimental implementations of active vibration damping and to compare quantitatively the experimental measurements of control system performance with theoretical predictions.

The general method of active vibration control called variously modal-space control, independent modal-space control (IMSC), and natural control has been developed by Meirovitch and his associates.[1,8] Since independence is generally unattainable in practice, and since the version of the method discussed herein is active damping rather than a more general type of control, the name modal-space active damping is most accurately descriptive here. As discussed in Ref. 7, the method is very closely related to a method of multiple-shaker modal excitation first described in 1950 by Lewis and Wrisley.[9]

The object of control is a flexible structure which is either being disturbed by environmental and/or maneuvering actions or is vibrating freely following such disturbances. It is presumed that the inherent passive damping is too light to adequately suppress the vibration, so that additional damping is required. Modal-space active damping is a method for producing this additional damping actively with the use of sensors, a feedback controller, and actuators; in the ideal case, it essentially provides a modal linear viscous dashpot individually to each vibration mode that requires active damping.

The authors have studied modal-space active damping because it is conceptually simple and it is well suited for comparison of experiment and theory. We do not necessarily advocate this control technique; we believe that insufficient information is available as yet to justify advocacy of any particular vibration control technique for large space structures.

II. Description of Modal-Space Active Damping

Consider a structure idealized to be linear with viscous inherent damping that does not couple the undamped normal modes of vibration. Suppose that one knows the natural frequencies and mode shapes of a particular set of n_c modes which are to be actively damped, the controlled modes, and that one has available n_a independently controllable actuators at specified positions on the structure. It will be specified in this theoretical development that the number of actuators equals the number of modes to be controlled, $n_a = n_c$. Suppose further that one wishes to impose the actuator forces and/or moments in order to affect each of the controlled modes independently of all other controlled modes.

If the structure is represented theoretically as an N-degree-of-freedom (DOF) finite-element model, the matrix equation of motion in physical coordinates is:

$$[m]\ddot{q} + [c]\dot{q} + [k]q = e(t) + c \tag{1}$$

The $N \times N$ matrices $[m]$, $[c]$, and $[k]$ are mass, noncoupling inherent viscous damping, and stiffness matrices, respectively; $q(t)$ is the vector of all time-dependent DOF, consisting of grid point translations and rotations; $e(t)$ is the vector of all possible grid point excitations, consisting of discrete forces and moments; and c is the vector of all possible grid point control actions.

Standard structural dynamics eigenanalysis decouples the left-hand side of Eq. (1), giving the modal equations of motion,

$$[M]\ddot{\xi} + [C]\dot{\xi} + [K]\xi = [\Phi]^T[e(t) + c] \tag{2}$$

Submitted March 5, 1984; presented as Paper 84-1018 at the AIAA Dynamics Specialists Conference, Palm Springs, Calif., May 17-18, 1984; revision submitted Aug. 10, 1984.

*Associate Professor, Aerospace and Ocean Engineering. Member AIAA.

†Graduate Research Assistant, Aerospace and Ocean Engineering. Student Member AIAA.

where $[\Phi]$ is the $N \times N$ modal matrix whose columns are mode shape vectors; the modal coordinates $\xi(t)$ are related to the physical coordinates $q(t)$ through the modal transformation, $q = [\Phi]\xi$; and the generalized mass, inherent viscous damping, and stiffness matrices are

$$[M] = [\Phi]^T[m][\Phi] = \text{diag}(M_r, r = 1,2,\ldots,N)$$

$$[C] = \text{diag}(2M_r\zeta_r\omega_r, r = 1,2,\ldots,N)$$

$$[K] = \text{diag}(M_r\omega_r^2, r = 1,2,\ldots,N)$$

where ω_r and ζ_r denote, respectively, the natural frequency and inherent viscous damping factor of the rth mode.

The n_a actuators are applied at points and in directions corresponding to a specific subset q^a of DOF. Accordingly, the $n_a \times 1$ actuator submatrix of c is denoted as c^a, all other elements of c being zero. Hence, Eq. (2) can be written as

$$[M]\ddot{\xi} + [C]\dot{\xi} + [K]\xi = [\Phi]^T e(t) + [\Phi^a]^T c^a \tag{3}$$

where the $n_a \times N$ matrix $[\Phi^a]$ consists of the appropriate rows of $[\Phi]$.

Feedback control vector c^a depends on the measured motion, so, in general, it can be a function of all ξ_j's and/or their derivatives. This paper considers only velocity feedback so that $c^a = c^a(\dot{\xi})$.

The essence of modal-space active damping is the selection of c^a in order to decouple that portion of the right-hand side of Eq. (3) associated with the specified controlled modes. The matrix equation describing only the controlled modes is

$$[M^c]\ddot{\xi}^c + [C^c]\dot{\xi}^c + [K^c]\xi^c = [\Phi^c]^T e(t) + [\Phi^{ac}]^T c^a(\dot{\xi}^c) \tag{4}$$

where superscript c denotes appropriate partitions of the matrices in Eq. (3); in particular, matrix $[\Phi^{ac}]$ is square (since it has been specified that $n_c = n_a$) and consists of the columns of $[\Phi^a]$ associated with the controlled modes.

Use of the form $c^a(\dot{\xi}^c)$ in Eq. (4) presumes that it is possible at least to estimate with reasonable accuracy the instantaneous modal velocity of each of the controlled modes. The present authors have chosen to do this by measuring physical response with a single sensor at a point which is nonnodal for all controlled modes and by directing this signal through parallel narrow-band spectral filters, one centered at the natural frequency of each controlled mode, to separate the response into individual modal contributions. (Meirovitch et al.[1] have used another type of response observer, a spatial modal filter, that requires several sensors but no spectral filtering.) Suppose that an ideal velocity sensor is placed at, say, the ith DOF. The output of this sensor is

$$\dot{q}_i(t) = \sum_{j=1}^{N} \dot{q}_{ij} = \sum_{j=1}^{N} \Phi_{ij}\dot{\xi}_j$$

Suppose that this output is directed through n_c ideal spectral filters, as described above. The ideal filter for a mode would introduce no phase lag and would have a sufficiently narrow passband and sufficiently steep rolloffs to completely exclude response from all other modes. Hence, the output of the filter for mode s is $\Phi_{is}\dot{\xi}_s$, and the collective output of all the controlled mode filters is $\dot{q}_i^c = [\Phi_i^c]\dot{\xi}^c$, where $[\Phi_i^c] = \text{diag}\,(\Phi_{is}, s$ over the controlled modes).

Considering again Eq. (4), one defines as A_s^a the unknown (at this point) apportioning of control actions which will isolate controlled mode s from all other controlled modes. If only the sth mode were to require control in the form of modal viscous damping, then one would produce that control by feeding back to the structure control actions of the form $c^a = A_s^a\dot{q}_{is}$. However, to suppress independently all of the controlled modes, one must use the summation

$$c^a = \sum_{s}^{n_c} A_s^a\dot{q}_{is} = [C^{ac}]\dot{q}_i^c \tag{5}$$

where $[C^{ac}]$, whose sth column is A_s^a, is the square control apportioning matrix. Hence, the matrix equation describing the controlled modes can be written as

$$[M^c]\ddot{\xi}^c + [C^c]\dot{\xi}^c + [K^c]\xi^c = [\Phi^c]^T e(t) + [\Phi^{ac}]^T[C^{ac}][\Phi_i^c]\dot{\xi}^c \tag{6}$$

In order for Eq. (6) to be fully uncoupled and to have a specified degree of active viscous damping in each controlled mode (in addition to the inherent damping), it is necessary that

$$[\Phi^{ac}]^T[C^{ac}][\Phi_i^c] = -[D^c] \tag{7}$$

where $[D^c] = \text{diag}(D_s = 2M_s\zeta_s^c\omega_s,\ s$ over the controlled modes), and ζ_s^c is the viscous active damping factor specified for mode s. Hence, the control apportioning matrix is the solution of Eq (7),

$$[C^{ac}] = -[\Phi^{ac}]^{-T}[D^c][\Phi_i^c]^{-1} \tag{8}$$

provided that the inverse matrices exist. Substituting Eq. (8) into Eq. (6) gives the uncoupled scalar equation governing each controlled mode,

$$M_s\ddot{\xi}_s + (C_s + D_s)\dot{\xi}_s + K_s\xi_s = \phi_s^T e(t)$$

s over the controlled modes, where ϕ_s is column s of $[\Phi]$.

Clearly, the ideal control apportioning of Eq. (8) allows each controlled mode to be suppressed independently of all other controlled modes. Note, however, that this control apportioning generally produces excitation of all modes other

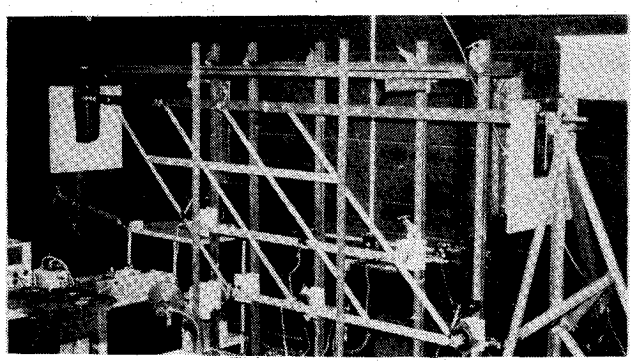

Fig. 1 Photograph of plane grid and support framework.

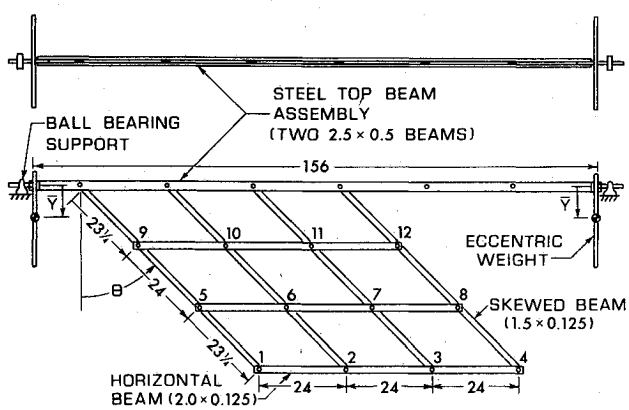

Fig. 2 Line drawing of plane grid (dimensions in in.).

than the controlled modes, which are called residual modes. One can demonstrate this by substituting Eqs. (8) and (5) into Eq. (3) and observing that the right-hand-side terms due to control in the scalar equations of motion for all residual modes are, in general, nonzero. This control spillover into the residual modes is a consequence of the presence of fewer control actuators than structural modes, and it can seriously impair control effectiveness.[10] There are also other practical factors that can influence effectiveness, including imperfect knowledge of modal parameters and nonideal sensing, filtering, and actuation. The effects of nonideal filtering and inaccuracies in theoretical models are of particular interest in this paper.

III. Plane Grid Laboratory Structure

Most previously reported experimental studies of active vibration control have considered relatively simple one-dimensional laboratory structures, primarily beams. (The study described in Ref. 2 was one of the few exceptions; in probably the most ambitious experiment reported to date, control was implemented on a three-dimensional spacecraft structure.) However, beam structures generally cannot exhibit some of the dynamic characteristics that may complicate active damping of large space structures, such as high model density and complex patterns of nodal lines. The plane grid illustrated in Figs. 1 and 2 was designed to provide these characteristics in a small laboratory structure. Details of its design and theoretical modeling are given in Refs. 11 and 12. Only relevant aspects of those reports are summarized herein.

The basic structure was a combination of highly flexible aluminum grid beams, a horizontal steel top beam assembly supported in nearly frictionless bearings, and rigid eccentric weights. Grid skew angle θ and eccentricity $\bar{Y}$ of the rigid weights were variable. For this paper, $\theta = 46$ deg and $\bar{Y} = 8.5$ in. Grid members were bolted together tightly at joints, 12 of which are labeled on Fig. 2.

The principal dynamic response of the plane grid consisted of out-of-plane motion. The structure had a dozen out-of-plane vibration modes with natural frequencies under 10 Hz, including a very low-frequency pendulum mode (the frequency of which was strongly dependent on $\bar{Y}$), and a pair of modes with closely spaced frequencies around 3.5 Hz. Natural frequencies and nodal lines were measured accurately in sine dwell modal tests with the use of noncontacting exciters (see Secs. V and VI) in single-point and two-point excitation configurations. Nodal points were detected by a noncontacting, inductive-type proximity probe (with 0.3-in. probe tip diameter), which was moved along the aluminum beams by a finely adjustable traverse mechanism.[12] Measured natural frequencies are listed in Table 1, and nodal lines (interpolated through measured points) for modes 2-5 are shown on Fig. 3.

Two refined finite-element models of the plane grid were evaluated.[12] Three DOF were assigned to each analysis grid point (node)—translation out of the plane, rotation about a vertical in-plane axis, and rotation about a horizontal in-plane axis. The first model was of lower order and consisted of analysis grid points at each of the 12 bolted joints of the aluminum grid, at the two bearing supports of the steel top beam, and at six points in the interior of the steel top beam; with three DOF per grid point and with out-of-plane translation prevented at each bearing support, this model had 58 DOF. In the second model, each beam between adjacent bolted joints of the aluminum grid was represented as two finite elements of equal length, rather than one; otherwise, it was identical to the first model. Consequently, the second model had 121 DOF. Corresponding natural frequencies calculated for the two finite-element models differ by less than 1% for all modes under 10 Hz, and corresponding calculated nodal points representative of the mode shapes are also nearly identical. One concludes, therefore, that for practical purposes the 58-DOF model converged mathematically for modes under 10 Hz.

Natural frequencies are listed for the 121-DOF model in Table 1 (and for the 58-DOF model in Table 2), and nodal lines for modes 2-5 of the 121-DOF model are shown on Fig. 3. An ad hoc, nonrigorous representation of the effects of gravity on the grid beams was required to make the theoretically calculated fundamental (pendulum) frequency match the experimentally measured value.[12] Comparison of experimental and theoretical natural frequencies in Table 1 shows good agreement, especially for modes 1-8. Experimental and theoretical nodal lines also match reasonably well for all of modes 1-8, except as shown on Fig. 3a, mode 2. This mismatch and the ad hoc treatment required for calculation of the correct pendulum frequency indicated that the finite-element model was deficient in some respect. The deficiency was discovered after completion of all experiments and calculations for this paper: A consistent beam geometric stiffness matrix[13] is required to account correctly for all the effects of gravity on the grid beams.

IV. Active Damping Configuration

The active damping task attempted was to provide $\zeta_s^c = 0.1$, $s = 2$-6; that is, it was desired to produce 10% active damping in modes 2-6 of the plane grid. Hardware availability limited the number of controlled modes to five. Modes 4 and 5 were included among the controlled modes because their frequencies were close to each other. The other modes were chosen, somewhat arbitrarily, to complete a sequence of adjacent low-frequency modes that did not include the fundamental (pendulum) mode.

The single control sensor was positioned at bolted joint 1 to measure out-of-plane translational velocity. This location was selected because theoretical mode shapes indicated that it was a point of substantial response for all of the controlled modes.

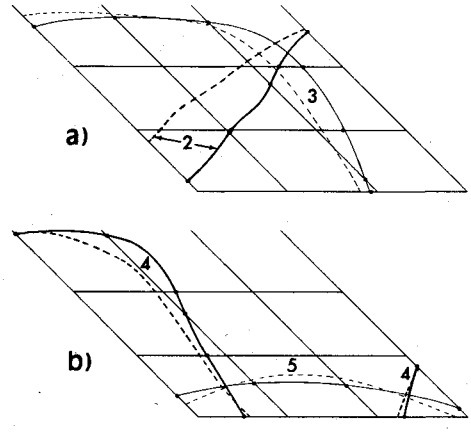

Fig. 3 Experimental (solid) and theoretical (dashed) nodal lines for a) modes 2 and 3, and b) modes 4 and 5.

Table 1 Plane grid natural frequencies

Structure mode	Natural frequency, Hz	
	Experimental	Theoretical
1	0.60	0.60
2	0.95	0.96
3	1.44	1.43
4	3.42	3.40
5	3.65	3.72
6	5.15	5.16
7	5.48	5.49
8	5.67	5.67
9	6.27	6.59
10	8.25	8.54
11	8.36	8.75
12	9.47	9.77

Table 2 Open- and closed-loop system roots

System root	Open-loop system			Structure-control systems: Five-mode control		Four-mode control	
	Type[a]	ζ_r	f_{or}(Hz)	ζ_r	f_{or}(Hz)	ζ_r	f_{or}(Hz)
1	SM 1	0.043	0.597	0.153	0.421	0.152	0.421
2	SM 2	0.050	0.965	0.074	0.913	0.074	0.914
3	FM 2	0.518	0.965	0.425	1.296	0.425	1.294
4	SM 3	0.035	1.432	0.046	1.290	0.048	1.290
5	FM 3	0.349	1.432	0.221	1.809	0.219	1.798
6	SM 4	0.010	3.413	0.026	3.104	0.027	3.156
7	FM 4	0.049	3.413	−0.010	3.559	0.029	3.675
8	SM 5	0.009	3.728	0.068	3.561	0.009	3.728
9	FM 5	0.045	3.730	0.022	3.987	0.045	3.730
10	SM 6	0.013	5.151	0.058	4.680	0.056	4.654
11	FM 6	0.097	5.152	0.041	5.640	0.047	5.659
12	SM 7	0.0035	5.494	0.011	5.480	0.0068	5.478
13	SM 8	0.0030	5.667	0.0044	5.666	0.0041	5.666
14	SM 9	0.0060	6.630	0.0092	6.747	0.0080	6.658
15	SM 10	0.0060	8.618	0.0061	8.642	0.0060	8.615

[a]SM r denotes structure mode r; FM r denotes filter for structure mode r.

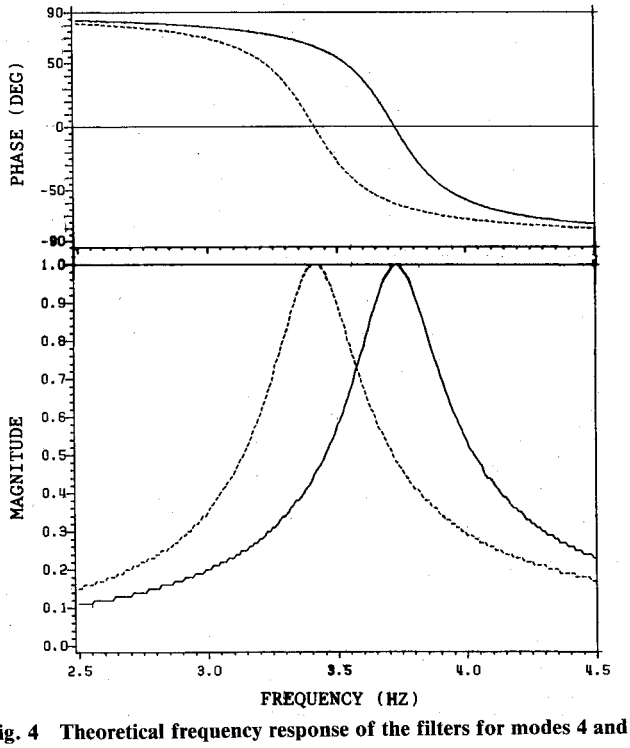

Fig. 4 Theoretical frequency response of the filters for modes 4 and 5.

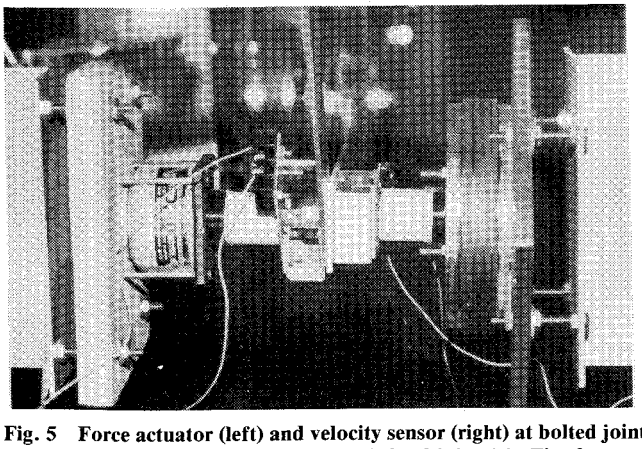

Fig. 5 Force actuator (left) and velocity sensor (right) at bolted joint 1 of the plane grid as viewed from the left of joint 1 in Fig. 2.

However, as was shown by subsequent measurements (Fig. 3a), bolted joint 1 was actually very close to a nodal line of mode 2.

Force actuators exerting control forces perpendicular to the plane were positioned at bolted joints 1, 2, 4, 5, and 8. These positions were selected in a semiquantitative manner rather than by mathematical optimization. The candidate positions were restricted to bolted joints 1-12, but joints 9-12 were eliminated because response of the controlled modes was generally much greater in the lower half of the plane grid. Equation (8) for control gain matrix $[C^{ac}]$ was evaluated with theoretical mode shapes for several different five-joint combinations from among joints 1-8. The combination 1, 2, 4, 5, and 8 was chosen because it produced the most uniform spatial distribution of control forces.

V. Control System Hardware

Active damping was effected by the velocity sensor, an analog controller, and the force actuators, all of which were custom designed and assembled in-house.

The control system implemented the version of Eq. (5) accounting for actual filter characteristics. The circuit design of the filters is that of Forward[4]; this design is analyzed in detail in Ref. 6. The response of the filter for controlled mode s is described by

$$\ddot{y}_s + B_s\dot{y}_s + \omega_{cs}^2 y_s = B_s\ddot{q}_i \tag{9}$$

where $\dot{q}_i$ is input, $\dot{y}_s$ output, B_s half-power bandwidth, and ω_{cs} passband center frequency. Hence, the version of Eq. (5) actually implemented is

$$c^a = \sum_{s}^{n_c} A_s^a y_s = [C^{ac}]y \tag{10}$$

Control gain matrix $[C^{ac}]$ was calculated from Eq. (8) with theoretical (rather than experimental) mode shapes.

Half-power bandwidth B_s was set at 1.00 Hz for modes 2, 3, and 6, and at 0.333 Hz for close modes 4 and 5. For each controlled mode, the filter center frequency was set at the mode's experimental (rather than theoretical) natural frequency. Figure 4 shows the frequency response functions calculated from Eq. (9) for modes 4 and 5.

The complete physical implementation of the active damping technique used in this study is summarized as follows. The velocity transducer provided sensor signal $\dot{q}_i$, and this signal was the input for the filter of each controlled mode. Im-

plementation of Eq. (10) consisted of three principal operations: 1) filter output y_s was multiplied into control gain vector A_s^a by a gain circuit; 2) the outputs from all gain circuits were added together by a summation circuit; and 3) each output of the summation circuit was directed into a power amplifier, which generated the input signal proportional to $c_j^a(t)$ for the jth control force actuator. It is noted for later reference that the control for any individual mode could be disabled by simply grounding the input to that mode's filter.

The analog controller, consisting of buffers, filters, and gain and summation circuits, was built around integrated circuit operational amplifiers.[6]

The velocity sensor and force actuators consisted of structure-borne conducting coils interacting with magnetic fields produced by stationary, noncontacting magnetic field structures[5] (Fig. 5). These devices were linear provided that coil displacement was less than about 2 mm from the static position. In order to minimize current flow in the velocity sensor coil (and hence additional but unwanted passive damping), it was necessary to pass the velocity signal into the filters through a unity gain buffer having extremely high input impedance.[6]

The power amplifiers driving the actuators were designed to have controlled current output; this was necessary to establish a linear transduction of summation circuit output voltage into actuator output force, eliminating the effect of voltage induced by motion of the actuator coil.[6]

VI. Experimental Procedure

Measured displacement-to-force frequency response functions (FRFs) were the principal type of experimental data used to evaluate the validity of the structure-control system theoretical model. The experimental procedure is summarized in this section, and the corresponding theoretical analysis is developed in Sec. VII.

Experiments were conducted with the use of an STI-11/23 data acquisition-analysis system developed by Synergistic Technology Incorporated, Cupertino, California. This system both generated the excitation signal and acquired and processed the data signals.

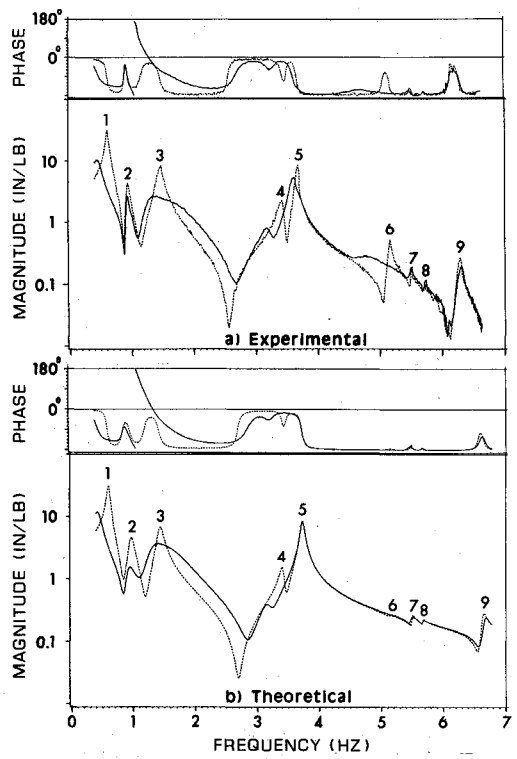

Fig. 6 Open loop (dashed) and closed loop (solid) FRFs of displacement at joint 2 due to excitation of joint 2. Resonance peaks of open loop structure modes are labeled by mode number.

Frequency response was measured directly in incremental sine sweeps. In such a sweep, an excitation signal is imposed at a driving frequency, and the force excitation and displacement response at that frequency are measured after a settling period in which transients are allowed to decay. The driving frequency is then changed by an increment and the process is repeated. The sweeps covered the 0.4-6.4 Hz range (including the nine lowest natural frequencies) in increments of 0.0122 Hz, generally taking 2-3 h.

It was necessary that dynamic displacements remain small in order not to exceed the ±2 mm linear range of the control sensor and actuators. Therefore, low-frequency excitation forces on the light and flexible plane grid had to be small. Even the smallest commercially available shakers and piezoelectric force gages proved too heavy-handed and insensitive for the task. However, the noncontacting force actuators provided a simple solution to the problem: In each frequency response sweep, the excitation signal from the STI-11/23 was added to the control feedback signal in the input to the power amplifier of a selected actuator. Thus, that actuator served simultaneously as the exciter and a control actuator. The excitation force was related through a calibration constant to the excitation signal. A typical force level required was on the order of 0.01 lb, and this was generated by an excitation signal on the order of 50 mV.[12] Because dynamic displacements were kept small, amplitude servocontrol was not required.

Frequency response displacements were measured at bolted joints of the plane grid by sensitive proximity probes (see Sec. III). Light 0.50 in.^{2} steel targets were used.

In order to minimize unwanted disturbances, it was necessary to conduct testing during periods of low personnel activity in the laboratory. Air currents produced by normal air conditioning, or by doors being opened and closed, or even by a person walking within a few feet of the plane grid could disturb the structure and reduce the quality of measured data.

VII. Theoretical Frequency Response and System Roots

The basic theoretical model of the complete structure-control system consists of the structural Eq. (1), n_c equations [Eq. (9)] describing the filters, and Eq. (10) for the vector of control actions.

The filter equations can be cast into the matrix form

$$[I]\ddot{y}+[B]\dot{y}+[\omega_c^2]y=[B][T_s]\ddot{q} \tag{11}$$

where y is the vector of n_c filter outputs, $[I]$ the identity matrix of order n_c, $[B]$ the diagonal matrix of filter half-power bandwidths, and $[\omega_c^2]$ the diagonal matrix of filter center frequencies squared. Also, $[T_s]$ is an $n_c \times N$ transformation matrix relating the sensor velocity $\dot{q}_i$ to the full velocity vector $\dot{q}$; accordingly, $[T_s]$ is null, except that column i (corresponding to DOF i) is a column of ones.

From Eq. (10), the vector of all N control actions, including $N-n_a$ zero elements is

$$c=[T_a][C^{ac}]y \tag{12}$$

where $[T_a]$, the $N \times n_a$ actuator transformation matrix, consists of appropriate zero and unit elements.

Now the complete, coupled physical system of order $N+n_c$ is described by the combination of Eqs. (1), (11), and (12). It is desirable to reduce the order of this system by assuming that structural response can be adequately described by a truncated set of n_t normal modes: $q=[\Phi^t]\xi^t$, where $[\Phi^t]$ and ξ^t are appropriate submatrices of $[\Phi]$ and ξ. Hence, the structural response is represented by the subset of modal Eq. (2),

$$[M^t]\ddot{\xi}^t+[C^t]\dot{\xi}^t+[K^t]\xi^t=[\Phi^t]^T(e+[T_a][C^{ac}]y) \tag{13}$$

where $[M^t]$, $[C^t]$, and $[K^t]$ are appropriate partitions of $[M]$, $[C]$, and $[K]$.

The vector of all retained modal coordinates and all filter outputs is defined as

$$z = \begin{bmatrix} \xi^t \\ y \end{bmatrix} \tag{14}$$

Combining Eqs. (11)-(14) into a single matrix equation of order $n_t + n_c$ gives

$$[AM]\ddot{z} + [AC]\dot{z} + [AK]z = f \tag{15}$$

where augmented mass, damping, and stiffness matrices are defined as

$$[AM] = \begin{bmatrix} [M^t] & [0] \\ -[B][T_s][\Phi^t] & [I] \end{bmatrix}, \quad [AC] = \begin{bmatrix} [C^t] & [0] \\ [0] & [B] \end{bmatrix}$$

$$[AK] = \begin{bmatrix} [K^t] - [\Phi^t]^T[T_a][C^{ac}] \\ [0] \qquad\qquad [\omega_c^2] \end{bmatrix}$$

and the augmented excitation vector is

$$f = \begin{bmatrix} [\Phi^t]^T e \\ 0 \end{bmatrix}$$

To calculate the FRF of displacement in any DOF for excitation in DOF k, one solves directly for $Z = [\Xi^T Y^T]^T$ using the form of Eq. (15),

$$([AK] - \omega^2[AM] + i\omega[AC])Z = F \tag{16}$$

where $i = \sqrt{-1}$ and $F = [E^T 0^T]^T$, in which E^T is the kth row of $[\Phi^t]$.

Calculation of the system complex roots (eigenvalues) is expedited by definition of the state vector $x = [\dot{z}^T z^T]^T$. Thus, one casts the homogeneous form of Eq. (15) into the state-space form $[SB]\dot{x} - [SA]x = 0$ where

$$[SB] = \begin{bmatrix} [0] & [I] \\ [AM] & [AC] \end{bmatrix}, \quad [SA] = \begin{bmatrix} [I] & [0] \\ [0] & -[AK] \end{bmatrix}$$

in which $[I]$ is the identity matrix of order $n_t + n_c$. Hence, the system roots are the complex eigenvalues p of

$$[SA]X = p[SB]X \tag{17}$$

For each complex conjugate pair $p = \sigma \pm i\omega$, one defines damping factor $\zeta = -\sigma/\sqrt{\sigma^2 + \omega^2}$ and frequency $f_0 = \sqrt{\sigma^2 + \omega^2}/2\pi$.

VIII. Experimental Results and Comparison with Theory

Figures 6 and 7 show two different FRFs, in measured and calculated versions, and for active damping turned off (open loop) and active damping turned on (closed loop). These two FRFs are the most illustrative of several that were evaluated.

To establish parameters of the theoretical model for use in numerical solutions of Eqs. (16) and (17), the open-loop experimental FRFs (dashed curves of Figs. 6a and 7a) were considered first. The open-loop theoretical model was produced by nulling the off-diagonal submatrices in augmented matrices $[AM]$ and $[AK]$, thus decoupling structure and filters. The ten lowest normal modes were used to represent the structure's dynamics, $n_t = 10$. The adequacy of this modal truncation was confirmed by comparison of experimental and theoretical results. Inherent damping matrix $[C^t]$ was estimated in a semiquantitative fashion: Modal inherent viscous damping factors ζ_r were adjusted iteratively until reasonable agreement in resonance peak magnitudes was achieved between measurements and calculations. Modal damping ratios estimated in this manner are listed in Table 2. Note that damping values for modes 1-6 are surprisingly high in view of the nature of the plane grid structure. These high values are almost certainly due to aerodynamic damping. A mathematical curve-fitting procedure would probably have produced more accurate modal damping values, because the method used did not account for mode shape errors in the theoretical results.

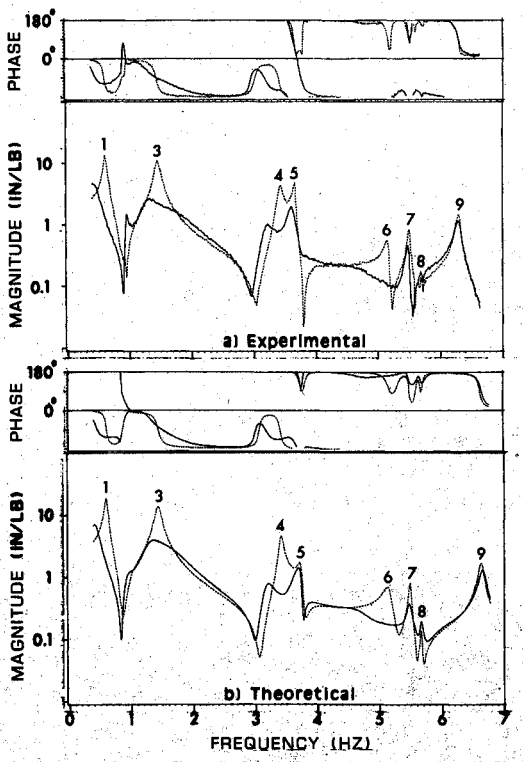

Fig. 7 Open loop (dashed) and closed loop (solid) FRFs of displacement at joint 5 due to excitation at joint 1. Resonance peaks of open loop structure modes are labeled by mode number.

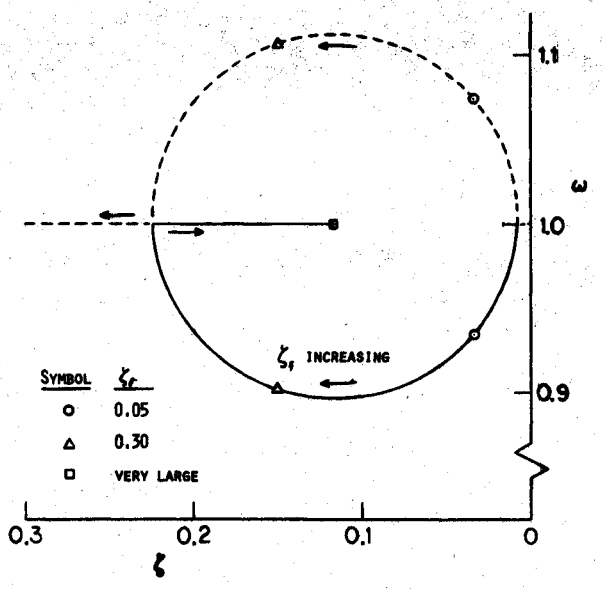

Fig. 8 Oscillator-filter loci of roots.

When five-mode active damping was activated, the structure-control system exhibited a mild dynamic instability at 3.55 Hz. It was determined by selective disabling of the controls for closely spaced modes 4 and 5 (see Sec. V) that, essentially, the control for mode 5 was driving mode 4 unstable. This circumstance is quite plausible in view of the considerable overlapping of the filter bandwidths for modes 4 and 5 (Fig. 4): Each of those modes could contribute significant, possibly destabilizing error signals to the input of the other mode's gain circuit. Roots calculated theoretically for the five-mode control are listed in Table 2. The single root with negative damping factor matches exactly the experimentally observed instability.

A stable structure-control system was produced by disabling the control for mode 5. Thus, the four modes 2, 3, 4, and 6 were actively damped by the five control actuators at bolted joints 1, 2, 4, 5, and 8. This is the system for which the closed-loop FRFs in Figs. 6 and 7 were measured and calculated and for which the four-mode control roots in Table 2 were calculated.

IX. Discussion of Results

Figures 6 and 7 show reasonable agreement between measurements and calculations. The differences are due primarily to errors in the theoretical mode shapes. One can see the effects of these errors, especially for modes 2 and 5, by examining the FRFs in light of the nodal lines on Fig. 3. Figure 6a shows that mode 2 received almost no active damping; this happened because the control gains were calculated on the basis of the theoretical shape of mode 2, which is significantly different than the actual shape. Note that mode 2 is not evident on either Fig. 7a or 7b because of nodal line locations: For Fig. 7a, the actual nodal line is close to joint 1, the excitation point; for Fig. 7b, the theoretical nodal line is close to joint 5, the response point.

Figures 6 and 7 indicate that four-mode active damping reduced substantially the resonance peak magnitudes of controlled modes 3, 4, and 6. It also provided unexpected additional damping to mode 1, which was not among the controlled modes; this damping was probably a modal rate feedback effect permitted by the 1-Hz half-power bandwidth of the filter for mode 2 (Sec. V).

There is a serious general discrepancy between the actual damping achieved, as represented adequately by the theoretical four-mode control roots in Table 2 and the active damping that was expected on the basis of the theory in Sec. II. The active damping factor specified for each controlled mode in the calculation of control gains was $\zeta_s^c = 0.10$; however, the damping factors achieved were much lower for all controlled modes. Observation of this discrepancy led to a search for an explanation, culminating in the analysis in the appendix of an oscillator (1-DOF structure) subjected to modal-space active damping with the use of a single spectral filter. The surprising and counterintuitive conclusion of the analysis is that, for practical purposes, the active damping actually achieved is a strong function of the filter half-power bandwidth, but is functionally independent of the specified active damping factor ζ^c.

Direct extrapolation of the result for the oscillator-filter system to the actual structure-control system is not appropriate because the filter bandwidths overlapped, and this certainly affected the damping achieved. However, it was relatively easy to simulate theoretically cases in which the filter bandwidths were made so narrow that they did not overlap. These calculations were performed for the five-mode control case. When all filter bandwidths were reduced in simulation to 10% of their actual values, the system became stable and each mode essentially had only its own inherent damping. This result substantiates the conclusion that filter bandwidth is the primary factor determining the degree of active damping achieved.

X. Concluding Remarks

The research reported herein evaluated a form of modal-space active damping that uses spectral filtering for modal estimation. It was demonstrated that the particular type of spectral filter used has a serious deficiency: In order to avoid instability due to mode-filter coupling, the bandwidth of the filter for a given controlled mode must be so narrow as to reject response from all other modes; however, by virtue of being narrow, the filter bandwidth can reduce the active damping to such a low level as to be useless.

Generally satisfactory agreement was achieved between experimental measurements and theoretical calculations. However, the nature of the inevitable differences observed suggests a practical guideline: Any active vibration control technique implemented on a dynamically complicated large space structure should be insensitive to errors in the structure model used to design the control, because that model is unlikely to accurately predict the parameters of all modes affected by the control.

Appendix: Oscillator-Filter System

Consider the case in which the structure is a simple 1-DOF damped oscillator with mass m, inherent viscous damping c, and stiffness k, and the filter has center frequency ω_f and half-power bandwidth B. For the version of modal-space active damping considered herein, the coupled structure-filter equations are

$$m\ddot{q} + c\dot{q} + kq = -dy, \qquad \ddot{y} + B\dot{y} + \omega_f^2 y = B\ddot{q}$$

where d is the active damping feedback constant. One defines structure natural frequency $\omega_s = \sqrt{k/m}$ and structure, filter, and active damping factors, respectively, $\zeta_s = c/2m\omega_s$, $\zeta_f = B/2\omega_f$, and $\zeta_a = d/2m\omega_s$.

The coupled equations become

$$\ddot{q} + 2\zeta_s\omega_s\dot{q} + \omega_s^2 q = -2\zeta_a\omega_s y$$

$$\ddot{y} + 2\zeta_f\omega_f\dot{y} + \omega_f^2 y = 2\zeta_f\omega_f\ddot{q}$$

Seeking solutions to these equations with time variation $\exp(\omega_s p t)$, one finds the following quartic characteristic equation for the dimensionless roots p,

$$(p^2 + 2\zeta_s p + 1)(p^2 + 2\zeta_f\Omega_f p + \Omega_f^2) + 2\zeta_a(2\zeta_f\Omega_f)p^2 = 0$$

where $\Omega_f = \omega_f/\omega_s$. If the roots are denoted $p = \sigma \pm i\Omega$, then the system damping factor and dimensionless frequency are $\zeta = -\sigma/\sqrt{\sigma^2 + \Omega^2}$ and $\omega = \sqrt{\sigma^2 + \Omega^2}$.

The variation of system roots with dimensionless filter bandwidth $B/\omega_s = 2\zeta_f\Omega_f$ is of interest. Numerical parameters representative of the cases considered in the main body of this paper are $\Omega_f = 1$, $\zeta_s = 0.016$, and $\zeta_a = 0.1$. For these parameters, the loci of roots having positive imaginary parts are shown in Fig. 8. Two ζ_f values are identified on the curved portions of the loci to illustrate a general observation: On these portions, the active damping factor ζ_a affects the system frequencies but has negligible influence on the system damping factors. These damping factors are equal and are approximated closely by $\zeta \simeq (\zeta_f + \zeta_s)/2$. The third point identified on the solid branch illustrates the other general observation: Only when the filter bandwidth becomes very large does the active damping factor take effect over system damping and provide the structure with the expected total damping factor $\zeta_a + \zeta_s$.

Acknowledgments

This work was supported by the U.S. Air Force Office of Scientific Research, Grant AFOSR-82-0217 and Contract F49620-83-C-0158. The data acquisition-analysis system was purchased with Grant No. CME-8014059 from the National

Science Foundation. Carolynn Russillo and David Russillo assisted greatly in the preparation of the manuscript.

References

[1]Meirovitch, L., Baruh, H., Montgomery, R.C., and Williams, J.P., "Nonlinear Natural Control of an Experimental Beam," *Journal of Guidance, Control, and Dynamics,* Vol. 7, No. 4, July-Aug. 1984, pp. 437-442.

[2]Bauldry, R.D., Breakwell, J.A., Chambers, G.J., Johansen, K.F., Nguyen, N.C., and Schaechter, D.B., "A Hardware Demonstration of Control for a Flexible Offset-Feed Antenna," *The Journal of the Astronautical Sciences,* Vol. 31, No. 3, July-Sept. 1983, pp. 455-470.

[3]Schaechter, D.B., "Hardware Demonstration of Flexible Beam Control," *Journal of Guidance, Control, and Dynamics,* Vol. 5, No. 1, Jan.-Feb. 1982, pp. 48-53.

[4]Forward, R.L., "Electronic Damping of Orthogonal Bending Modes in a Cylindrical Mast—Experiment," *Journal of Spacecraft and Rockets,* Vol. 18, No. 1, Jan.-Feb. 1981, pp. 11-17.

[5]Hallauer, W.L. Jr., Skidmore, G.R., and Mesquita, L.C., "Experimental-Theoretical Study of Active Vibration Control," *Proceedings of 1st International Modal Analysis Conference,* 1982, pp. 39-45.

[6]Skidmore, G.R., "A Study of Modal-Space Control of a Beam-Cable Structure," M.S. Thesis, Virginia Polytechnic Institute and State University, May 1983.

[7]Skidmore, G.R., Hallauer, W.L. Jr., and Gehling, R.N., "Experimental-Theoretical Study of Modal-Space Control," *Proceedings of 2nd International Modal Analysis Conference,* 1984, pp. 66-74.

[8]Meirovitch, L. and Oz, H., "Modal-Space Control of Large Flexible Spacecraft Possessing Ignorable Coordinates," *Journal of Guidance and Control,* Vol. 3, No. 6, Nov.-Dec. 1980, pp. 569-577.

[9]Lewis, R.C. and Wrisley, D.L., "A System for the Excitation of Pure Natural Modes of Complex Structures," *Journal of the Aeronautical Sciences,* Vol. 17, Nov. 1950, pp. 705-722 and 735.

[10]Hallauer, W.L. Jr. and Barthelemy, J.-F. M., "Sensitivity of Modal-Space Control to Nonideal Conditions," *Journal of Guidance and Control,* Vol. 4, No. 5, Sept.-Oct. 1981, pp. 564-566.

[11]Masse, M.A., "A Plane Grillage Model for Structural Dynamics Experiments: Design, Theoretical Analysis, and Experimental Testing," M.S. Thesis, Virginia Polytechnic Institute and State University, Feb. 1983.

[12]Gehling, R.N., "Experimental and Theoretical Analysis of a Plane Grillage Structure with High Model Density," M.S. Thesis, Virginia Polytechnic Institute and State University, March 1984.

[13]Argyris, J.H., Hilpert, O., Malejannakis, G.A., and Scharpf, D.W., "On the Geometrical Stiffness of a Beam in Space—A Consistent V.W. Approach," *Computer Methods in Applied Mechanics and Engineering,* Vol. 20, 1979, pp. 105-131.